

A FINITE-DIFFERENCE SIMULATION OF WAVE PROPAGATION IN TWO-DIMENSIONAL RANDOM MEDIA

BY ARTHUR FRANKEL* AND ROBERT W. CLAYTON

ABSTRACT

A finite-difference algorithm is used to generate synthetic seismograms for waves propagating through two-dimensional random media. The media have a significant component of their material properties varying randomly over length scales smaller than the seismic wavelength and are meant to approximate the heterogeneity of the crust and upper mantle. The finite-difference technique retains all multiply scattered and diffracted waves, and also accounts for transmission losses.

The synthetic seismograms clearly exhibit coda and apparent attenuation caused by scattering. For a medium with a white wavenumber spectrum of velocity fluctuations, the coda is higher frequency than the initial pulse. The apparent attenuation is greatest when the scatterer size is comparable to the seismic wavelength. The spectra of the coda generally increase in frequency as the scatterers decrease in size. Examples demonstrate how scattering can produce spectra with broad peaks and sharp fall-offs that can make the determination of the source spectra and corner frequencies of small earthquakes extremely difficult.

INTRODUCTION

The scattering of seismic waves has achieved particular attention in recent years as seismologists have attempted to analyze short-period seismograms ($T < 1$ sec) from earthquakes, explosions, and seismic exploration surveys. An improved understanding of the scattering process has direct application to many problems in seismology, including: the description of the small-scale heterogeneity of the earth; the determination of the mechanism of seismic attenuation at high-frequencies ($f > 1$ Hz) in the earth; and the correction for path effects from the waveforms and spectra of small earthquakes and explosions.

In this paper, we investigate wave propagation in two-dimensional random media using numerical simulations in order to better assess the effects of scattering in the real earth. The random media we consider here contain significant components of their material properties varying randomly in space. We apply a heterogeneous, finite-difference method to produce complete synthetic seismograms for these media. These synthetic seismograms allow us to deduce how the small-scale properties of a random medium affect measurable features such as amplitude, spectrum, and coda decay of short-period seismograms.

Of specific interest are random media with spatial fluctuations in their properties on a scale finer ($<$ a few kilometers) that can be deterministically measured from macroscale observations (e.g., seismic refraction or reflection surveys). Such fluctuations can be caused by lithologic changes and the presence of cracks and pore fluids. The existence of small-scale variations of velocity in the earth's crust is documented by well logs (c.f. O'Doherty and Anstey, 1971), phase and amplitude variations of teleseismic waves across seismic arrays (Aki, 1973), the presence of

*Present address: Jet Propulsion Laboratory, California Institute of Technology, Pasadena, California 91109.

seismic coda (Aki and Chouet, 1975), and a cursory examination of the heterogeneous nature of rock in outcrops.

This paper presents our initial work on this problem and demonstrates the applicability of the finite-difference technique to wave propagation in random media. The advantages of the finite difference method include: (1) it produces synthetic seismograms rather than just envelopes of waveforms; (2) it does not require many of the assumptions that are commonly invoked in theoretical studies of scattering such as the first Born approximation, and (3) it is not restricted to media with specific statistical properties.

The simplifying assumptions used in most studies of seismic scattering are that only single scattering occurs and that the scattered energy is much smaller than the incident energy so that transmission losses from the direct wave can be neglected. These assumptions comprise the first Born approximation and are only valid for weakly scattering media, and may not be appropriate for the earth's crust (see Hudson and Heritage, 1981). The Born approximation has been used in theoretical studies of the apparent attenuation of a scattering medium (see Chernov, 1960; Wu, 1982; Malin and Phinney, 1984) and in the analysis of the coda decay of microearthquakes (Aki and Chouet, 1975; Sato, 1977).

It is well known that scattering can produce apparent attenuation with many characteristics similar to intrinsic attenuation caused by such mechanisms as frictional sliding on cracks and fluid modes in porous media (Aki, 1980). One major question is whether seismic attenuation in the crust at high frequencies is dominated by scattering or by intrinsic dissipation. To resolve this question, it is necessary to identify differences between seismic waves and that have been attenuated by the two types of processes. Richards and Menke (1983) produced complete synthetic seismograms (including multiple scattering) for plane waves traveling at normal incidence through a stack of plane layers with randomly varying velocities. They demonstrated the characteristics of the apparent attenuation and coda decay that are manifested in such one-dimensional random media.

The finite-difference method retains all multiply scattered waves, incorporates transmission losses, and can produce synthetic waveforms for two-dimensional random media. In the sections that follow, we will briefly discuss the finite-difference technique and describe our preliminary findings concerning the apparent attenuation and the coda characteristics exhibited in the synthetics.

THE FINITE-DIFFERENCE TECHNIQUE FOR HETEROGENEOUS MEDIA

The finite-difference method used in this paper solves the heterogeneous, acoustic wave equation on a two-dimensional grid. The reader is referred to Boore (1972) and Kelly *et al.* (1976) for a more detailed description of the method. The acoustic wave equation in a heterogeneous medium can be expressed as

$$\frac{\partial^2 P}{\partial t^2} = K \nabla \cdot (\rho^{-1} \nabla P) \quad (1)$$

where P is the pressure, K denotes the bulk modulus and ρ represents the density. In this paper, we assume that the density is constant in the medium, so that equation (1) simplifies to

$$\frac{\partial^2 P}{\partial t^2} = v^2(x, z) \left[\frac{\partial^2 P}{\partial x^2} + \frac{\partial^2 P}{\partial z^2} \right] \quad (2)$$

where $v(x, z)$ is the wave velocity, which is an arbitrary function of position on the grid. The partial derivatives in equation (2) are replaced by their finite difference approximations for a grid spacing of $\Delta h = \Delta x = \Delta z$ and a time increment of Δt . We use fourth-order approximations for the spatial derivatives to achieve a higher degree of accuracy at short wavelengths. This point will be discussed later in this section.

Once equation (2) is expressed in terms of finite differences, the pressure at any point in the mesh at time $t_0 + \Delta t$ can be calculated from the values of pressure at that grid point at times t_0 and $t_0 - \Delta t$ and from the pressure at eight adjacent grid points at time t_0 . By performing successive iterations, the pressure field at each point in the grid can be explicitly determined for some future time, given an initial pressure distribution. Since the method solves the heterogeneous wave equation, it includes all multiply scattered waves, diffractions, and surface waves. It also accounts for all transmission losses, in contrast to the Born approximation.

Because the finite-difference technique approximates the temporal and spatial derivatives, inaccuracies result at short wavelengths (and high frequencies) where

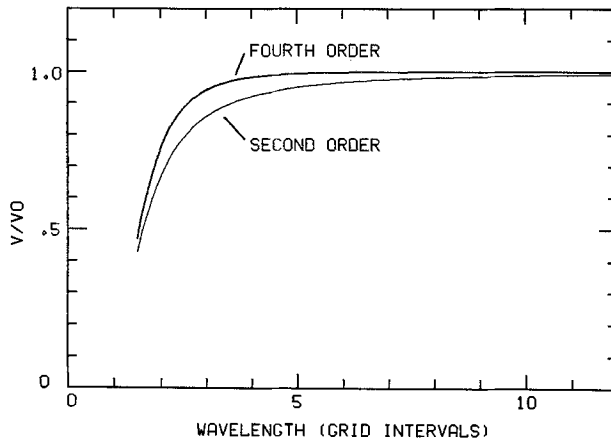


FIG. 1. Normalized phase velocity for the second and fourth-order finite-difference algorithms plotted as a function of wavelength (in units of grid intervals). The phase velocity v is normalized to the zero-frequency (errorless) phase velocity v_0 . These curves are for propagation parallel to the grid and stability ratios p of 0.5 for the second-order case and 0.325 for the fourth-order example. The curves were derived using the error analysis described in Alford *et al.* (1974).

these approximations become less accurate. The accuracy at a given wavelength is a function of the ratio of that wavelength to the grid spacing. The numerical inaccuracies can cause a frequency-dependent error in phase velocity known as grid dispersion (Alford *et al.*, 1974). For the fourth-order scheme used in this paper, Alford *et al.* (1974) demonstrated that a wavelength to grid spacing ratio of five or greater is required to achieve reasonable accuracies. Figure 1 illustrates the substantial reduction in phase velocity error of the fourth-order scheme relative to the second-order algorithm. At a given wavelength, the error varies somewhat with the value of the stability ratio $p = v\Delta t/\Delta h$ (Alford *et al.*, 1974). Since we are particularly concerned with maximizing the number of wavelengths that span the grid, we need to examine relatively high-frequency portions of the synthetics. Therefore, the fourth-order scheme represents an important improvement over the second-order algorithm. For stability the fourth-order approximation requires the time step to be smaller than $\sqrt{3/8}\Delta h/v_{\max}$, where v_{\max} is the maximum velocity in the grid (Alford *et al.*, 1974).

As a simple test of the accuracy of the finite-difference method, we constructed synthetic seismograms for the case of a plane wave propagating at normal incidence through a stack of plane layers with random velocities. The velocities were calculated by adding a random component to an average velocity of 3.25 km/sec (Figure 2). The finite-difference synthetics were compared to synthetics calculated using propagator matrices (Haskell, 1960). In this comparison, we used the heterogeneous *SH* wave equation for a medium with a constant shear modulus but a varying density. This equation is identical to equation (2) but with the *SH* displacement replacing the pressure. Synthetics were calculated for a receiver at the top of the layer stack (Figure 2). A Gaussian-shaped displacement pulse was incident at

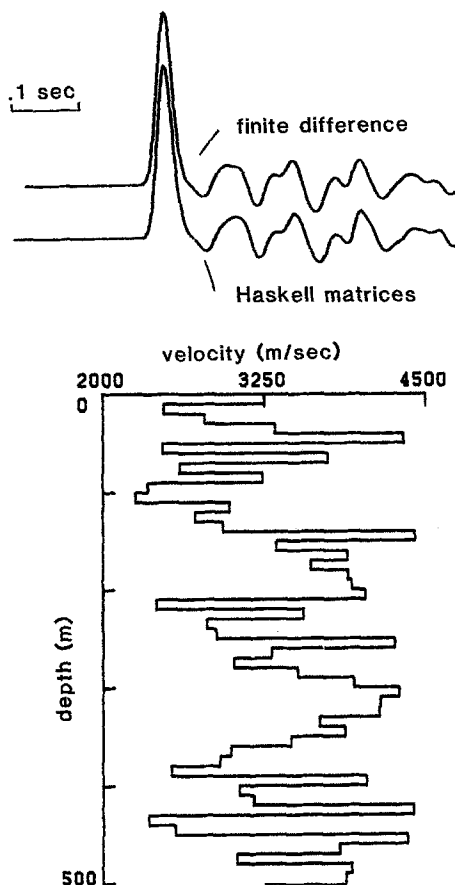


FIG. 2. Synthetics derived from the finite difference and Haskell matrix methods for a plane *SH* wave propagating vertically through a stack of plane layers. The receiver is at the surface. The velocities of the layers varied randomly as depicted at the bottom of the figure. The input waveform used to make both synthetics was shaped as a Gaussian.

the bottom of the stack. Fifty layers with randomly varying velocities, each 10 m thick, were considered (Figure 2). The grid spacing for the finite-difference run was set at 10 m so that the velocity varied at each grid point. The correlation between the two synthetics indicates that the fourth-order finite difference scheme has sufficient accuracy to model media with rapidly varying parameters.

SPECIFICATION OF THE RANDOM MEDIA AND THE SOURCE FUNCTION

The two-dimensional random medium was constructed by specifying a separate velocity for each grid point, consisting of a random component added to a constant,

average velocity. The random component has a Gaussian probability distribution. Figure 3 shows an example of the random portion of the velocity model. This random medium has a white wavenumber spectrum of velocity fluctuations.

The velocity model shown in Figure 3 can be interpreted as an approximation of a vertical cross-section of the earth's crust for body wave studies or of a plan view of scatterers for the investigation of regional phases such as L_g . We used an average velocity of 6.5 km/sec, a grid spacing of 20 m, and a time step of 1 msec. This yields

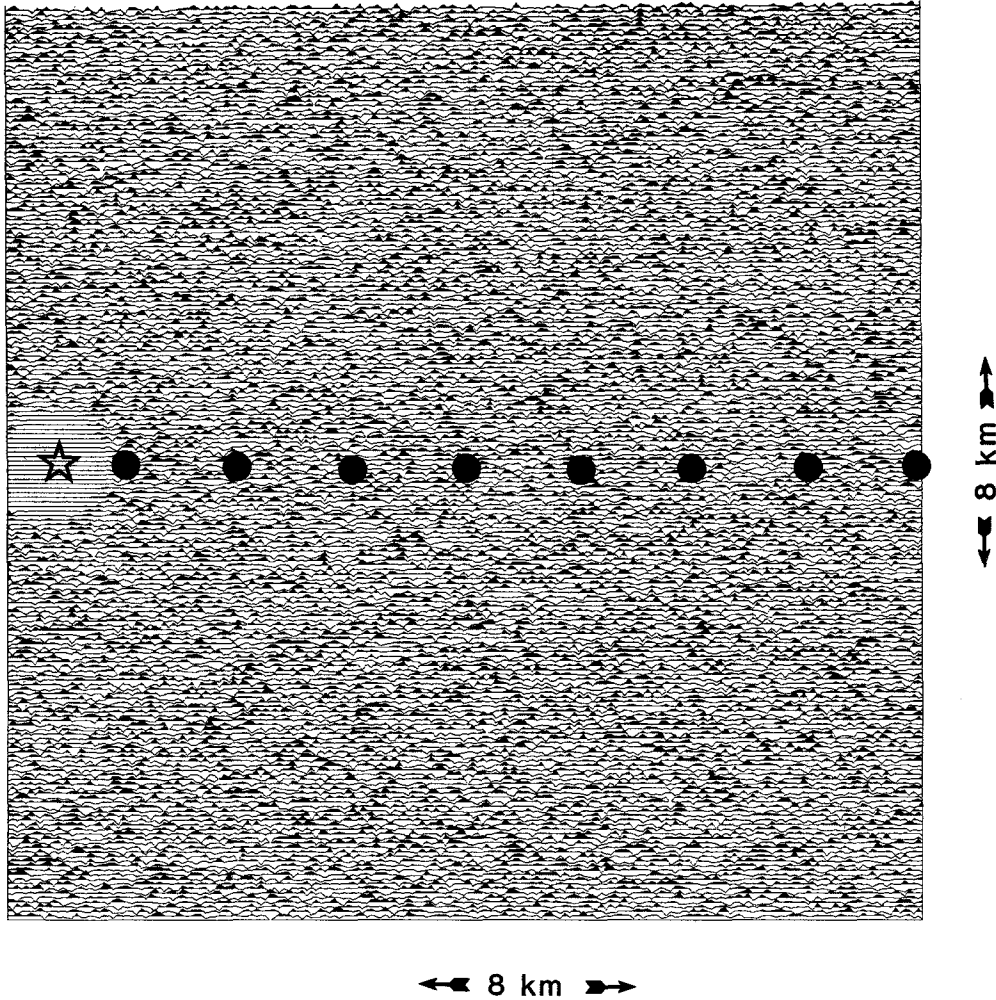


FIG. 3. Representation of the random component of a two-dimensional random medium. The amplitude of the horizontal lines indicates the random component of velocity at each grid point. Higher than average velocities are shaded, whereas areas with average or lower than average velocities are unshaded. The star denotes the source location and is surrounded by a circular, homogeneous area. The solid circles represent the receiver locations where the synthetic seismograms were calculated.

a stability ratio p of 0.325 at the average velocity. Since the grid size was 400 by 400 points, this artificial slice of the earth's crust is 8 km on a side, with a velocity that varies every 20 m. At the highest frequency examined in this paper, 35 Hz, the wavelength to grid spacing ratio is always larger than 5.5. Figure 3 also illustrates the configuration of the source and receivers used to make the synthetics shown in this paper. Artificial reflections from the sides, top, and bottom of the grid were

suppressed with the absorbing boundary conditions given by Clayton and Engquist (1977).

The source is centered in a circular, homogeneous portion of the mesh. The source is a line source of pressure that extends perpendicular to the plane of the grid. Our method of incorporating the source is based on Alterman and Karal (1968), except that we use a fourth-order algorithm. The time function of the source is

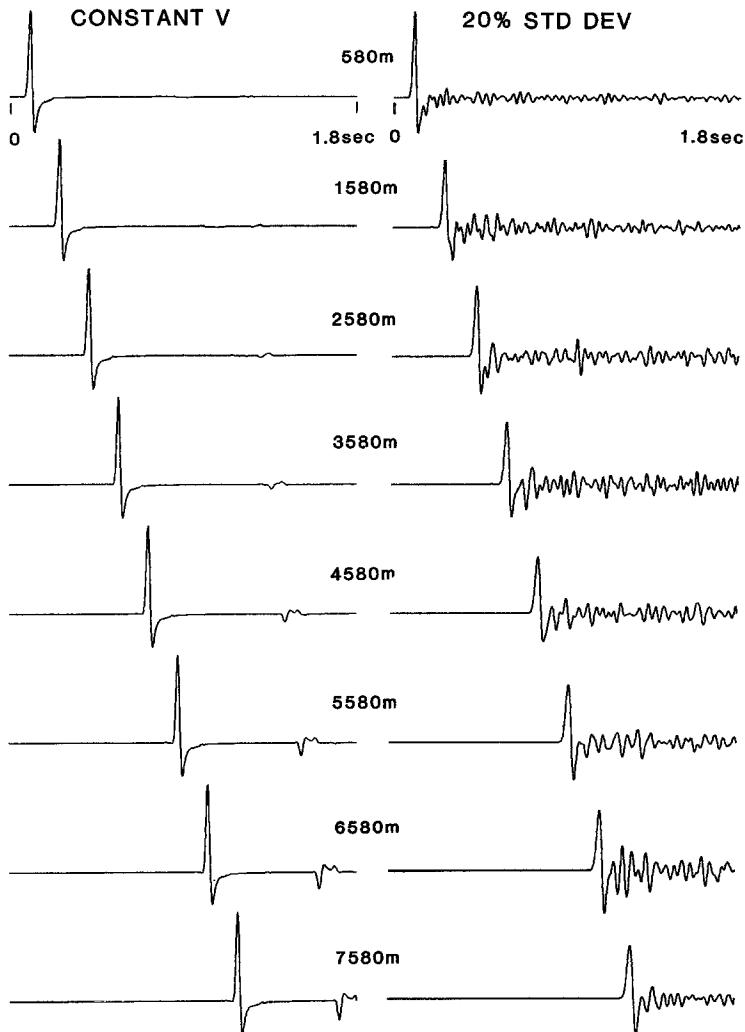


FIG. 4. (Left) Finite-difference synthetics at receivers between 580 and 7580 m from the source for a constant velocity grid. Amplitudes of all synthetics shown in this paper are corrected for geometrical spreading. (Right) Finite-difference synthetics for a random medium with a 20 per cent standard deviation in velocity.

chosen so as to produce a band-limited spectrum. We used a source time function that was the first derivative of a Gaussian (Alford *et al.*, 1974). The pulse width can be varied to represent different source durations.

APPARENT ATTENUATION FROM SCATTERING

The left side of Figure 4 shows the synthetic seismograms obtained for a grid with a constant velocity of 6.5 km/sec. The amplitudes of all of the synthetics

shown in this paper have been corrected for geometrical spreading (multiplied by $distance^{1/2}$). The receiver configuration is depicted in Figure 3. The source pulse propagates through the grid without a noticeable change of shape, indicating that the grid dispersion is insignificant. The small secondary arrivals observed on the more distant receivers are residual artificial reflections from the top and bottom of the grid.

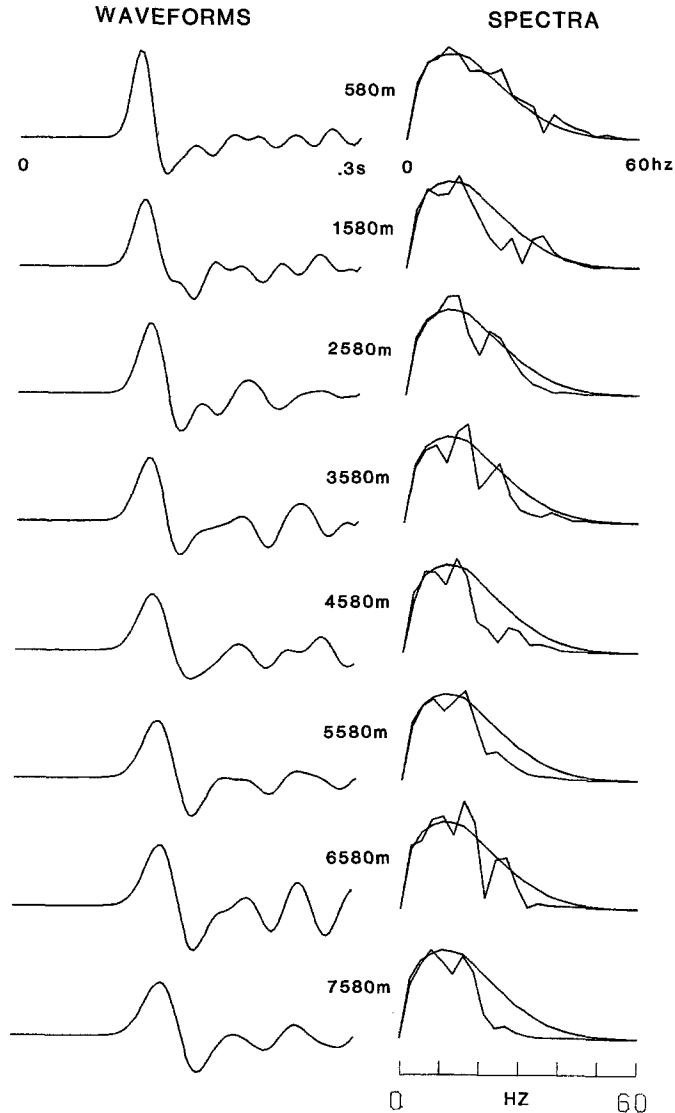


FIG. 5. (Left) Initial portions of synthetics from the right side of Figure 4 displayed on an expanded time scale and aligned in time. (Right) Spectra for the waveforms shown to the left on linear axes of amplitude and frequency. The smooth spectrum in each panel is from the initial pulse from the constant velocity synthetics. Amplitudes of waveforms and spectra are corrected for geometrical spreading.

On the right side of Figure 4, we display the finite difference synthetics for a random medium with a 20 per cent standard deviation in velocity. The synthetics exhibit significant amounts of coda from scattered waves arriving after the initial pulse. There is a distinct decrease in the amplitude of the initial pulse between the first two stations that is also visible on the more distant stations. The geometrical

spreading correction is a constant multiplicative factor applied to each trace so that the amplitudes of the initial pulses can be compared. Since the travel distances of the coda waves differ from the initial pulses, this correction is not appropriate to adjust the coda amplitude for geometrical spreading.

The behavior of the initial pulses can be observed in more detail in Figure 5, which shows the synthetics on an expanded time scale. It is clear that the amplitude of the pulse has decreased between the first two stations and that the pulse has broadened. In fact, the pulse width measured at the half-height of each pulse systematically increases with distance.

The spectra on the right half of Figure 5 were derived from the waveforms to the left. The spectral amplitudes were also corrected for geometrical spreading. The smooth spectrum in each panel represents the spectrum of the pulse for the case of the constant velocity grid. Figure 5 demonstrates that the spectra generally are depleted in high-frequency energy (>20 Hz) relative to the constant velocity case as the distance increases.

All of the above-mentioned features of the synthetics for the random medium: amplitude decay of the initial pulse, broadening of the pulse, and loss of high-frequency energy, are manifestations of the apparent attenuation produced by scattering. We should emphasize that intrinsic attenuation has not been included in these simulations, so that all amplitude losses are caused by scattering.

To further investigate both the apparent attenuation of the initial pulse and the coda decay, we bandpassed the synthetics for the random medium at two center frequencies (Figure 6). The filters used were zero phase Butterworth filters. Figure 6 also includes the envelopes for the filtered waveforms. The amplitude of the high-frequency portion (25 to 35 Hz) of the initial pulse varies considerably between receivers, although there is a general trend of decreasing amplitude with distance.

In order to adequately quantify the apparent attenuation of the initial pulse in a random medium, it is necessary to produce synthetic seismograms for media with a variety of random velocity sequences. Finite-difference synthetics were produced for two other sets of random media, each with 20 per cent standard deviations in velocity. The maximum amplitudes of the envelopes of the high-frequency portion of the initial pulse (25 to 35 Hz) were measured for the three simulations. The amplitudes A were expressed as fractions of the amplitude at the nearest receiver (A_0) and were plotted against receiver distance on a log-linear graph (Figure 7). When the envelope amplitudes from the three runs are considered together, there is an exponential decay of amplitude with distance, with significant variability in the amplitudes at any given distance. The apparent Q can be calculated from the slope of this decay by

$$Q = \frac{\omega}{2} \left[\frac{-D}{v \ln(A/A_0)} \right], \quad (3)$$

where D is travel distance, ω denotes the angular frequency, and v is the average velocity. The decay rate for random media with 20 per cent standard deviation in velocity yields a scattering Q of 82 ± 14 at 30 Hz.

Amplitude decay measurements were also taken from waveforms produced in random media with other standard deviations in velocity, σ (Figure 7). We determined apparent Q values of 150 and 340 for media with 14 and 10 per cent standard deviations, respectively. Thus, the apparent attenuation appears to be proportional

to the variance (σ^2) of the velocity, consistent with theoretical results for single scattering (Wu, 1982; Menke, 1983; Malin and Phinney, 1984).

These examples demonstrate that scattering in a two-dimensional random medium can produce large amounts of attenuation with several characteristics similar

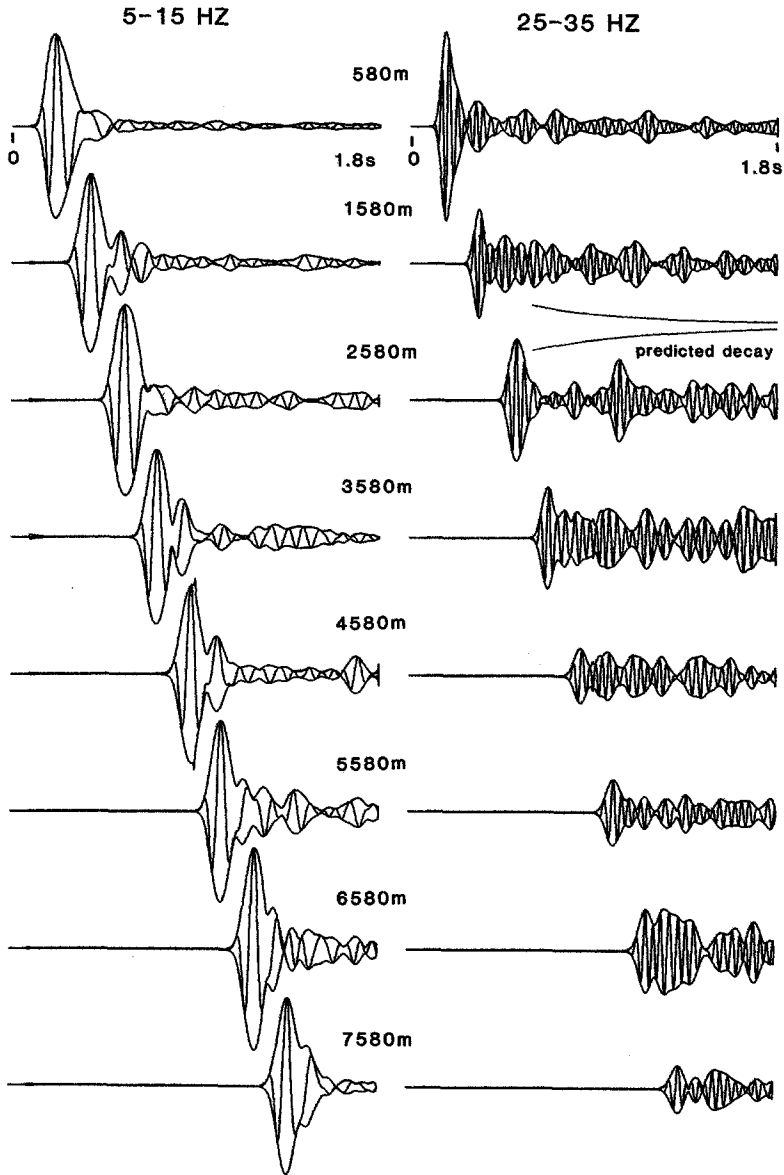


FIG. 6. Synthetic waveforms from the right side of Figure 4 bandpassed by phaseless filters between the indicated frequencies. Envelopes of waveforms are also plotted. All amplitudes are corrected for geometrical spreading. Also shown is a coda envelope with the decay rate predicted by the single scattering model of Aki and Chouet (1975) for an apparent Q of 82.

to intrinsic attenuation. For realistic values of standard deviation in velocity (≈ 10 per cent), it is clear that scattering can account for a substantial portion of the attenuation values commonly reported for short-period seismic waves in the crust ($Q \approx 200$ to 500). For a given variance of velocity, random media with different

correlation distances (i.e., scatterer sizes) will produce different amounts of attenuation at a particular frequency. This point will be addressed in a later section.

The large variability in the envelope amplitude of the initial pulse emphasizes the difficulty of determining the coefficient of apparent attenuation in scattering media. Figure 8 shows the synthetics for a random medium with a different sequence of velocities than that used to produce Figures 4 to 6. In the center of Figure 8, we depict the spectra of the initial pulses superimposed with the spectra of the pulses from the case of a constant velocity medium. The spectral amplitudes at 10 Hz for the random medium synthetics at 6580 and 7580 m are larger than those of the constant velocity case. This implies that multipathing has an important effect on the amplitude of the initial pulse in a scattering medium.

CODA

The finite-difference synthetics also provide useful information about the frequency content and time decay of the coda that follows the initial pulse. The frequency content of the coda clearly differs from that of the initial pulse. The right

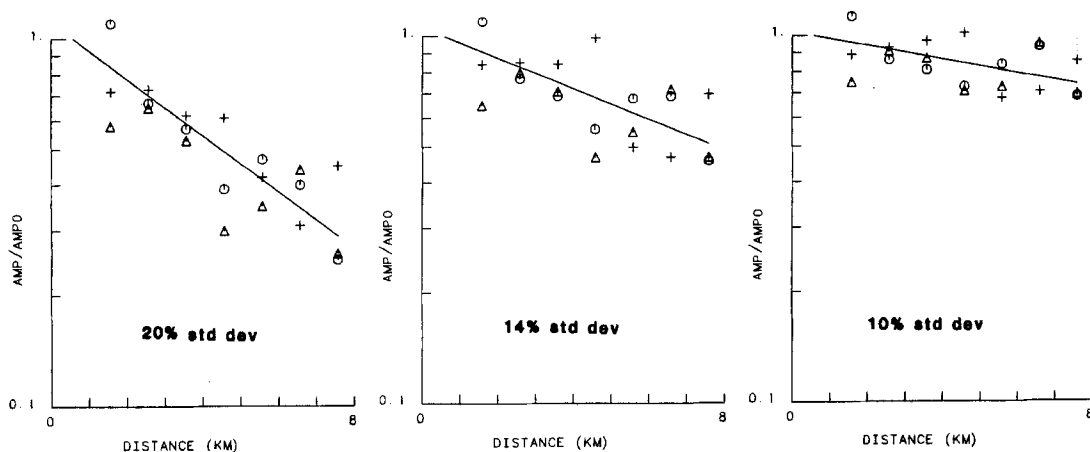


FIG. 7. Relative amplitudes of the envelopes of the 25 to 35 Hz waveforms plotted against distance for synthetics generated in random media with standard deviations in velocity of 20, 14, and 10 per cent. Each symbol signifies the measurements taken from the synthetics for a particular random sequence. The lines indicate the best-fit decays constrained to pass through unit amplitude at a distance of 580 m.

side of Figure 8 displays the spectra of the coda. Whereas the maximum energy of the initial pulse is at about 10 Hz, the coda energy is generally peaked between 15 and 30 Hz. We find this feature in the synthetics for all the simulations with this type of random medium. Because there is no intrinsic loss of energy, the high-frequency energy depleted from the direct wave by the scattering attenuation must become part of the scattered wave field. Thus, we would expect the coda to be enriched in high-frequency energy relative to the initial pulse. This characteristic of scattering attenuation was reported for one-dimensional random media by Richards and Menke (1983).

Differences in the frequency content of the coda and the initial pulse have been observed for the *P* waveforms from certain microearthquakes in the northeastern Caribbean (Frankel, 1982). Figure 9 shows the *P* waveform for a magnitude 1.9 event recorded by a short-period seismometer ($f_0 = 1$ Hz) 31 km away. The direct pulse has its peak spectral amplitude at about 11 Hz, whereas the coda spectrum is greatest at approximately 20 Hz. This observation implies that the characteristics

of scattering attenuation found in the synthetics can be identified in microearthquake waveforms.

We have made some preliminary comparisons between the coda decay of the synthetics and that derived from the single back-scattering model proposed by Aki and Chouet (1975). The coda decay predicted by this model for a Q of 82 and frequency of 30 Hz is shown in the right half of Figure 6. At receiver-source distances of 1580 and 3580 m, the coda of the synthetics appear to decay at a slower

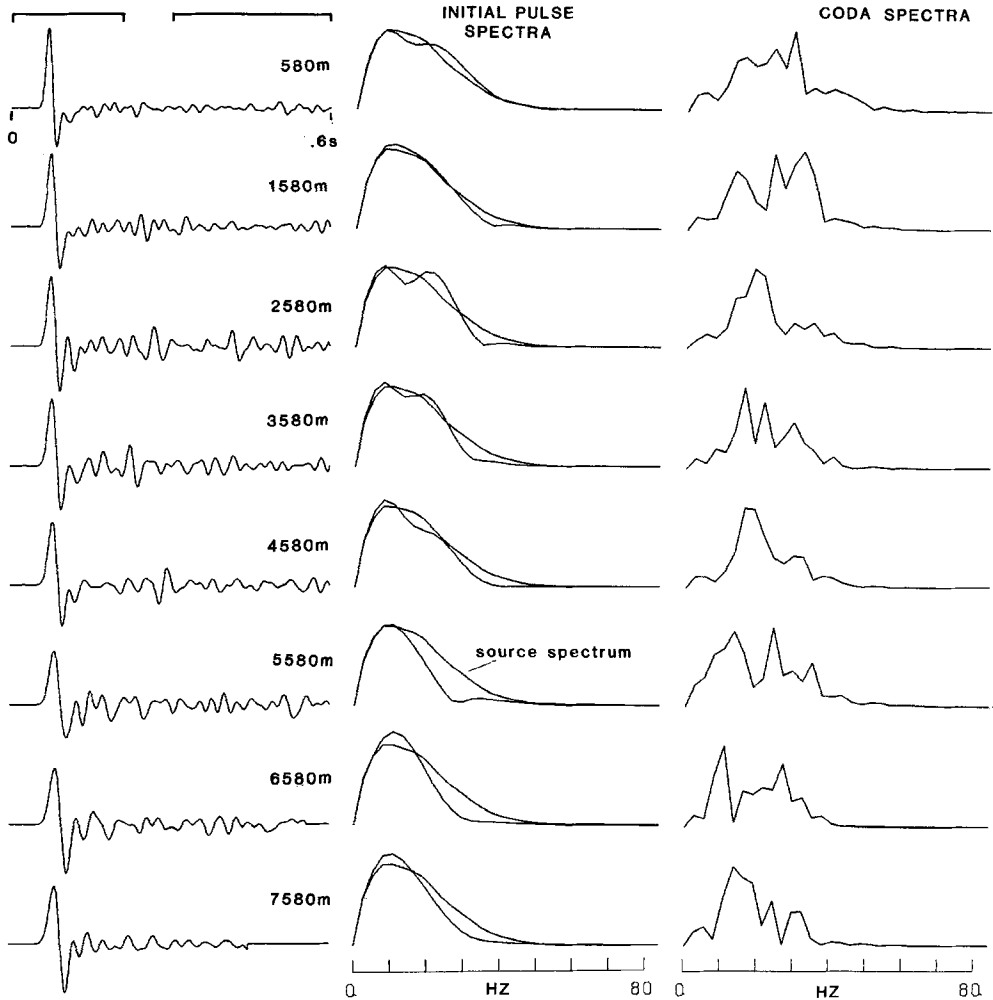


FIG. 8. (Left) Synthetics produced for a random medium with a 20 per cent standard deviation in velocity constructed with a different random number sequence than used to make the waveforms in Figure 4. Bars above the waveform indicate the time windows chosen to compute the spectra shown to the right. (Center) Spectra of the initial portion of the synthetics. The smooth spectra are the spectra from the constant velocity case. (Right) Spectra of the coda.

rate than predicted from the single scattering model. Gao *et al.* (1983) and Richards and Menke (1983) reported that the inclusion of multiple scattering produced a more gradual coda decay than the single scattering theory. The relatively slow rate of decay in some of the synthetics indicates that multiple scattering is important to the coda formation, at least for random media with 20 per cent standard deviation in velocity. Further work is required to quantify the effects of multiple scattering on the coda decay.

EFFECTS OF SCATTERER SIZE

One central question concerning scattering is: what can the characteristics of the apparent attenuation and the frequency content of the coda reveal about the size distribution and fluctuation amplitude of scatterers in the crust? The ratio between the wavelength of the seismic wave (λ) and the size of the scatterer (a) is of critical importance in the physics of the scattering process (see Aki, 1980). To study this problem, we bandpass-filtered the random velocity grid so that only narrow ranges of scatterer sizes were retained. This was accomplished by calculating the two-dimensional Fourier transform of the random number grid, zeroing the Fourier coefficients for the wavenumbers that were not desired, and performing the inverse transform back into spatial coordinates.

Figure 10 contains the synthetics obtained for media with three different ranges of scatterer sizes. The media were all normalized after filtering so that the standard

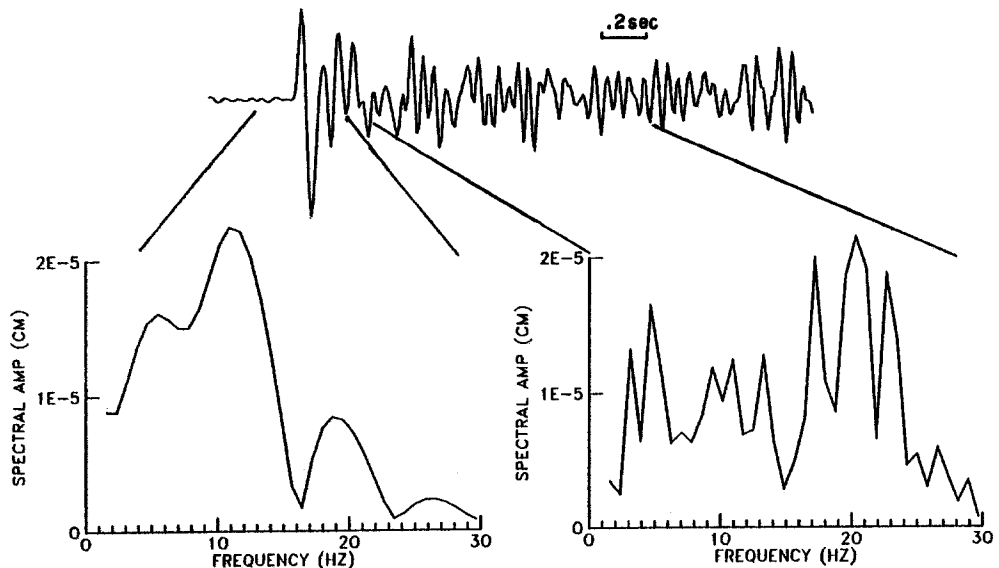


FIG. 9. *P* waveform of a magnitude 1.9 event in the northeastern Caribbean recorded at a station of a local seismic network ($\Delta = 31$ km), along with velocity spectra of the initial pulse and coda (from Frankel, 1982). Note that the coda is higher frequency than the initial pulse.

deviation of velocity was 20 per cent of the average velocity. The source pulse was identical for each run and had a peak frequency which corresponded to a wavelength of about 600 m. When the scatterer size a is slightly less than the dominant wavelength of the pulse ($a = 350$ to 450 m), the initial pulse is drastically attenuated with distance. At distances of 1580 m and greater, the initial pulse is usually not the largest arrival in the seismogram. The initial pulse is less attenuated with distance for the case when the scatterers are significantly smaller than the pulse wavelength ($a = 150$ to 250 m). The attenuation of the initial pulse is even less pronounced when the scatterers are between 50 and 150 m in size, much smaller than the pulse wavelength.

The dependence of attenuation on a/λ can also be recognized by bandpassing the synthetics in Figure 10 between 25 and 30 Hz so that the dominant wavelength of the seismic waves is about 235 m (Figure 11). When the scatterers are larger than this wavelength, $a/\lambda = 1.7$, there is a decrease of amplitude of the initial pulse

with distance. For this case, the peak amplitudes of the filtered waveforms occur significantly after the initial pulse. When $a/\lambda = 0.85$, a consistent and dramatic decrease in the amplitude of the initial pulse occurs with increasing distance. The peak amplitudes of these waveforms are found in the coda. The attenuation of the initial pulse with distance becomes noticeably less severe when the scatterers are

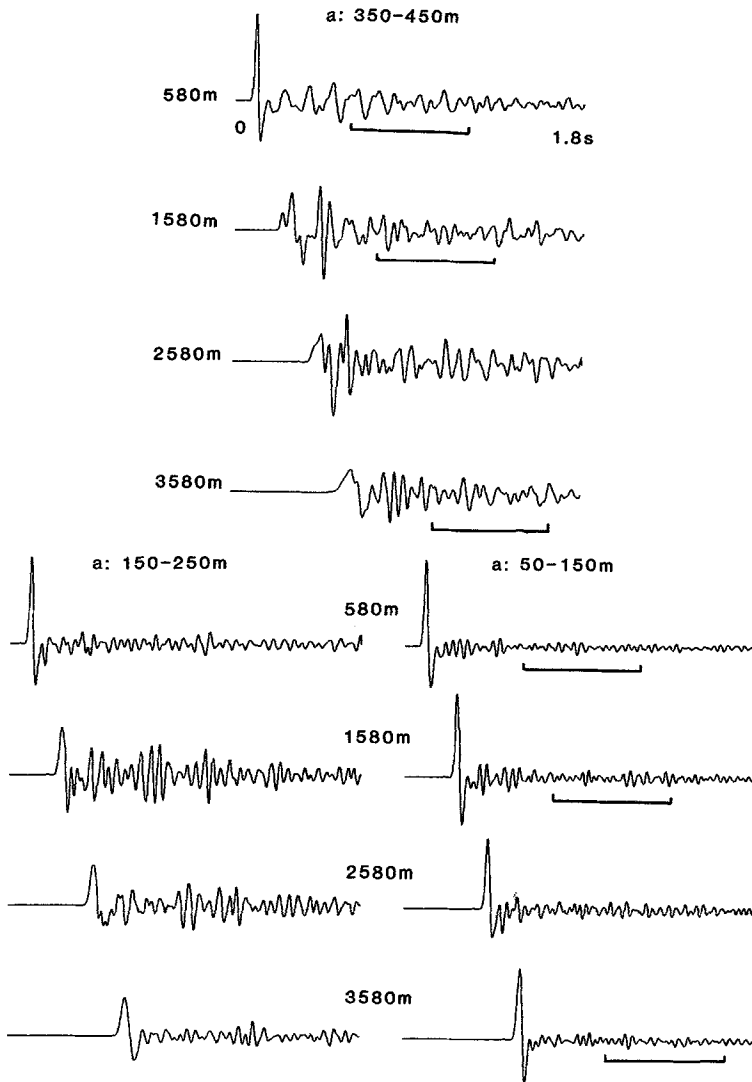


FIG. 10. Finite-difference synthetics obtained for three media with different ranges of scatterer size (a). Each medium had a 20 per cent standard deviation in velocity. Waveforms at four receivers are shown for each medium. All amplitudes are corrected for geometrical spreading. Bars indicate the time windows used to calculate the coda spectra in Figure 12.

much smaller than the seismic wavelength ($a/\lambda = 0.42$). Figures 10 and 11 both demonstrate that the apparent attenuation is largest when the scatterer size is comparable to the seismic wavelength. This characteristic was also found in synthetics generated for filtered media with other random velocity sequences. This relation between attenuation and the wavelength to scatterer size ratio is qualita-

tively consistent with the theoretical results derived from the single scattering assumption (Wu, 1982; Malin and Phinney, 1984).

The frequency content of the coda is also a function of the size of the scatterers. Figure 12 illustrates the spectra taken from the coda of the waveforms shown in Figure 10. It is clear that the coda produced by the medium with smaller scatterers

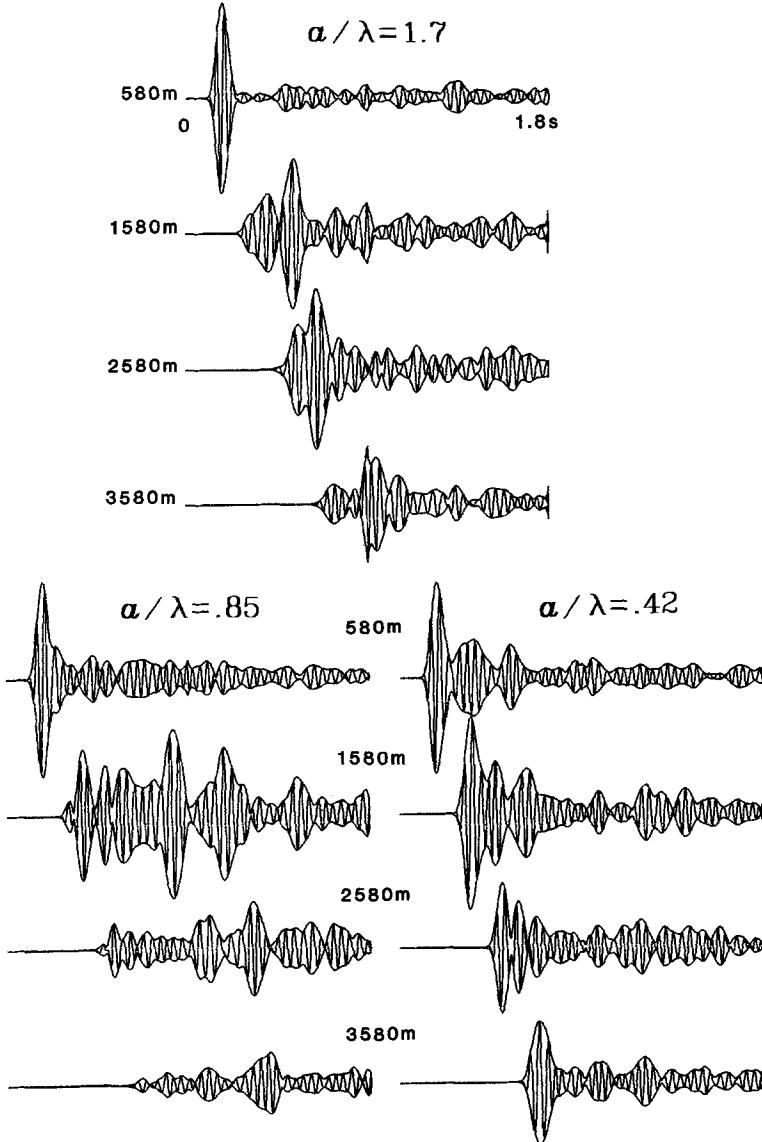


FIG. 11. Synthetics of Figure 10 bandpass-filtered between 25 and 30 Hz. a/λ denotes the ratio between scatterer size and seismic wavelength.

($a = 50$ to 150 m) is generally higher frequency than that generated by the medium with scatterers between 350 and 450 m in size. This observation can be understood in light of the findings about the apparent attenuation in bandpassed media presented above. Since the apparent attenuation is greatest when the scatterer size is comparable to the seismic wavelength, the smaller scatterers will selectively

remove energy at higher frequencies from the initial pulse, relative to the larger scatterers. This relatively high-frequency energy scattered by the smaller scatterers will be distributed into the coda, causing the coda from the small scatterers to be higher frequency than that from the larger ones.

The spectral content of seismic coda may provide useful information about the size of scatterers in the earth's crust. Of course, if intrinsic attenuation is significant, the coda spectra will be lower frequency than expected from the scatterer size. Furthermore, the high-frequency energy of the coda will be limited by the source characteristics.

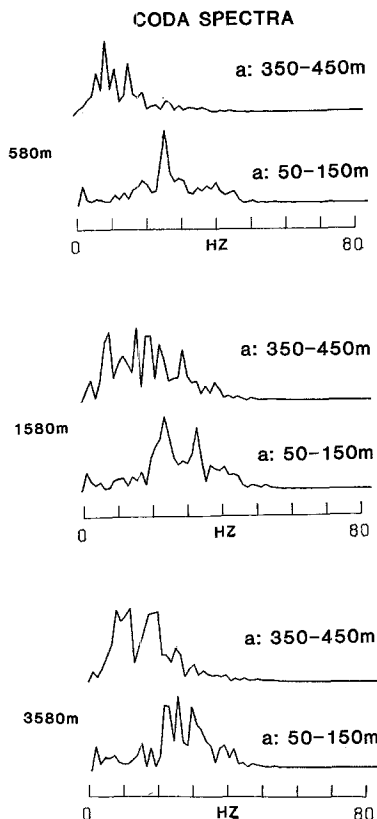


FIG. 12. Coda spectra calculated from the waveforms shown in Figure 10 for media with different ranges of scatterer size a . In each case, coda spectra are compared at the same receivers, whose distances from the source are indicated on the left.

IMPLICATIONS FOR THE DETERMINATION OF MICROEARTHQUAKE SOURCE SPECTRA

One major problem in the estimation of source parameters of small earthquakes ($M < 4$) is that their source durations (and hence dimensions) must be determined from spectral corner frequencies or pulse widths that are strongly distorted by scattering. This problem is illustrated in Figure 13, which contains spectra from finite-difference synthetics computed for random media with the white wavenumber spectra constructed with two different random number sequences. Both simulations used identical source durations, source-receiver configurations and standard devia-

tions in velocity (20 per cent). The spectra were calculated from the entire portion of the synthetics, including both the initial pulse and the coda.

The spectra at a given receiver can be remarkably different for the two media. The scattering produces broad spectral peaks and sharp cut-offs that vary between receivers and between the two media. For example, it would be difficult to have

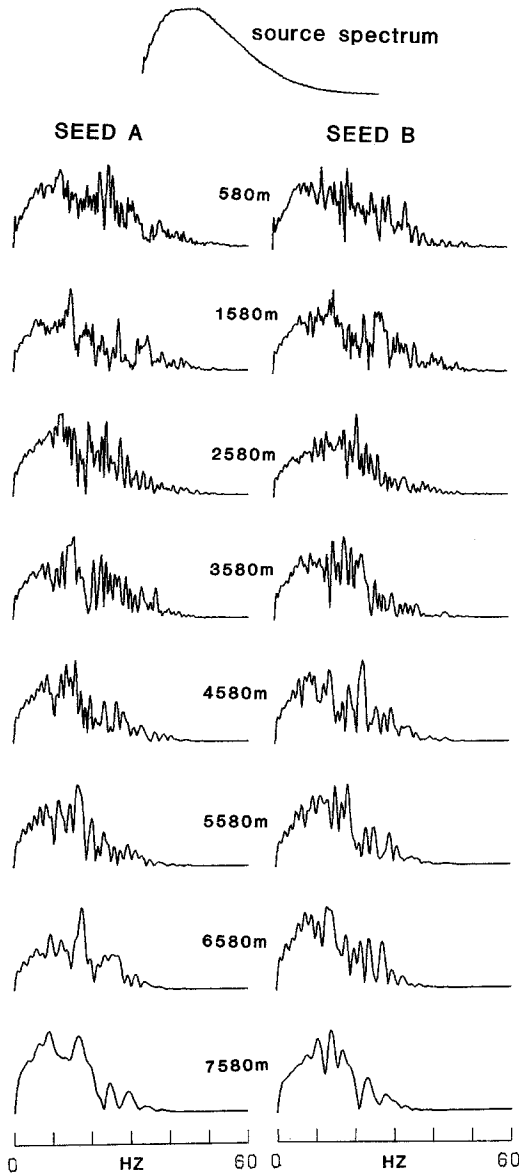


FIG. 13. Spectra calculated from synthetic seismograms for random media generated with two different random number sequences (20 per cent standard deviation). Source spectra and source-receiver geometry were identical in both runs. The spectra are normalized to their peak amplitudes.

deduced a priori that the spectra at the receivers at 4580 m distance were produced by the same source, particularly if the waveforms were recorded on an instrument with a narrow bandwidth. The spectral peaks and cut-offs represent the transfer function of the scattering medium for that particular source receiver combination

and that particular random sequence of velocities. These features are caused by the random, constructive, and destructive interference of various scattered waves arriving in the initial pulse and the coda. The synthetic spectra are analogous to the velocity spectra of earthquakes, with the peak frequency corresponding approximately to the corner frequency of the displacement spectrum. This experiment illustrates the difficulty of estimating the source corner frequencies of microearthquakes from receivers at different locations in a scattering medium.

An interesting similarity can be observed between the synthetic seismograms and actual microearthquake waveforms for the case of two spatially coincident sources with differing source durations. In Figure 14, we depict the synthetic seismograms

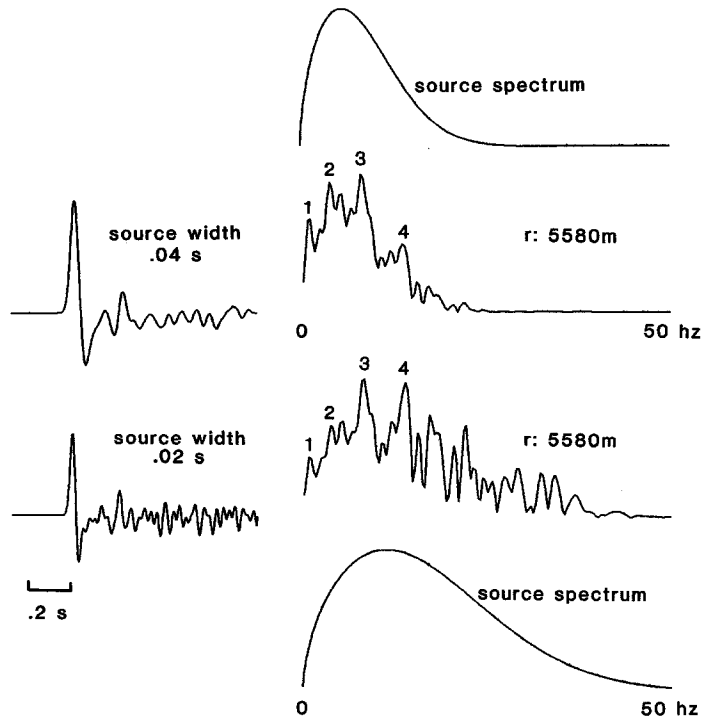


FIG. 14. Synthetic waveforms and spectra derived for sources of different pulse widths embedded in the same random medium (20 per cent standard deviation). Spectra and waveforms are from the receiver 5580 m from the source. Note the correspondence of the numbered peaks in the two spectra despite the overall difference in the source spectra.

and spectra obtained for sources with different durations (0.02 and 0.04 sec) embedded in the same random medium at the same location. Despite the variation in source spectra, the peaks and troughs of the spectra from the synthetics correspond between the two simulations. These features represent the transfer function of the scattering medium, whereas the difference in overall frequency content is caused by the difference in source spectrum.

The presence of peaks produced by scattering is also exhibited in the spectra of two adjacent microearthquakes in central Asia (Figure 15). These events occurred near the Toktogul Reservoir and were recorded by a local seismic network described in Simpson *et al.* (1981). The earthquakes were located within 500 m of each other and had local magnitudes of 1.7 and 0.9. As in the case of the synthetic spectra of Figure 14, the spectra contain several spectral peaks which correlate between the two earthquakes. The relative amplitudes of the peaks differ between the two events, with the smaller event exhibiting more energy at higher frequencies.

We contend that the spectral peaks observed in Figure 15 are produced by scattering effects. It can be argued that the spectral peaks between 15 and 20 Hz in Figure 15 correspond to a characteristic barrier size common to the fault zone of both events (Papageorgiou and Aki, 1983). In this interpretation, the rupture zone

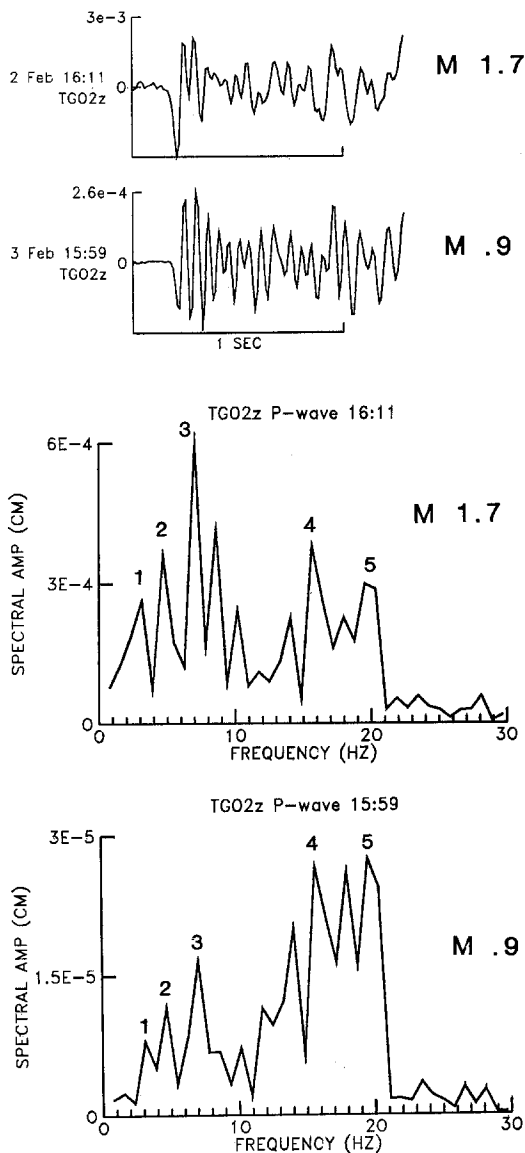


FIG. 15. *P* waveforms and velocity spectra of two adjacent microearthquakes (magnitudes 1.7 and 0.9) near the Toktogul Reservoir in central Asia recorded at a nearby station ($\Delta = 5.6$ km) of a local seismic network. Waveform amplitudes are expressed in centimeters/second. The spectra were not corrected for the low-pass filters in the instrumentation, so that spectral amplitudes greater than 20 Hz are somewhat underestimated. Note the correlation of the numbered peaks in the spectra of the two events.

of the smaller earthquake would be limited to a single barrier spacing. Spectral peaks 1, 2, and 3 observed in the spectrum of the larger event would represent the overall source dimension of that earthquake, rupturing across several barriers. However, peaks 1, 2, and 3 are also observed in the spectra of the smaller event. It

is physically unreasonable for the smaller earthquake to contain spectral peaks characteristic of the source size of the larger one. Therefore, the numbered peaks in Figure 15 are probably caused by scattering and not by source properties. The overall variation in the frequency content of the spectra is produced by differences in the source spectra, as with the synthetic spectra in Figure 14.

This example points out the importance of using small earthquakes as empirical Green's functions to identify and correct for the transfer function of the scattering medium before the source spectra of larger events are determined. Without examining the spectrum of the small event, the spectral peaks 4 and 5 observed for the larger earthquake in Figure 15 could have been misidentified as features of the source spectrum rather than as scattering resonances. Another path effect that has not been explicitly considered here is the site response, which is the severe attenuation that can occur at shallow depths (<3 km) beneath the receiver sites (see, Frankel, 1982; Hanks, 1982; Waller and Malin, 1983). This attenuation may be caused by scattering or by intrinsic dissipation and must also be corrected for when estimating the source spectra of microearthquakes (see Frankel and Kanamori, 1983).

DISCUSSION

In this paper, we have presented, in a generally qualitative manner, our initial results of numerical simulations of wave propagation in two-dimensional random media. We have demonstrated that the finite-difference technique is a useful method for studying scattering. The observations of the apparent attenuation, the variability of amplitudes, and the frequency content and time decay of the coda will be quantified in future work.

We would expect that the scattering phenomena found here for two-dimensional media would also occur in three-dimensional random media, with some quantitative differences. Scattering attenuation would probably be greater in three-dimensional random media than in two-dimensional media with similar velocity variations, since additional energy could be scattered out of the plane depicted in Figure 3. Two competing processes would change the coda amplitude and decay rate in three-dimensional random media from those in two-dimensional ones: a larger number of possible scatterers over the initial wavefront at any given time and a more rapid decay in amplitude from geometrical spreading (see, Aki and Chouet (1975) for the case of single scattering).

The utility of the finite difference method used here is that it allows the investigator to perform numerical experiments by changing the characteristics of the random medium and then measuring the properties of the resulting synthetic seismograms. Future extensions of this work include the use of elastic finite-difference codes and the incorporation of intrinsic absorption. The final goal of this effort will be the application of these numerical experiments to the quantitative interpretation of actual short-period seismograms.

ACKNOWLEDGMENTS

We thank William Menke and Peter Malin for useful discussions about scattering. The microearthquake data from the Toktogul network (Figure 15) were analyzed while one of the authors (A.F.) was a research associate at the Lamont-Doherty Geological Observatory. The research for this paper was supported by a grant from the Sun Oil Company. A.F. was supported by a postdoctoral Bantrell Fellowship.

REFERENCES

- Aki, K. (1973). Scattering of *P* waves under the Montana LASA, *J. Geophys. Res.* **78**, 1334–1346.
- Aki, K. (1980). Scattering and attenuation of shear waves in the lithosphere, *J. Geophys. Res.* **85**, 6496–6504.
- Aki, K. and B. Chouet (1975). Origin of coda waves; source, attenuation and scattering effects, *J. Geophys. Res.* **80**, 3322–3342.
- Alford, R. M., K. R. Kelly, and D. M. Boore (1974). Accuracy of finite difference modeling of the acoustic wave equation, *Geophysics* **39**, 834–842.
- Alterman, Z. S. and F. C. Karal, Jr. (1968). Propagation of elastic waves in layered media by finite-difference methods, *Bull. Seism. Soc. Am.* **58**, 367–398.
- Boore, D. M. (1972). Finite-difference methods for seismic wave propagation in heterogeneous materials, in *Methods for Computational Physics*, vol. 2, B. Alder, S. Fernbach and M. Rotenberg, Editors, Academic Press, New York.
- Chernov, L. A. (1960). *Wave Propagation in a Random Medium*, McGraw-Hill Book Co., Inc., New York.
- Clayton, R. and B. Engquist (1977). Absorbing boundary conditions for acoustic and elastic wave equations, *Bull. Seism. Soc. Am.* **67**, 1529–1540.
- Frankel, A. (1982). The effects of attenuation and site response on the spectra of microearthquakes in the northeastern Caribbean, *Bull. Seism. Soc. Am.* **72**, 1379–1402.
- Frankel, A. and H. Kanamori (1983). Determination of rupture duration and stress drop for earthquakes in Southern California, *Bull. Seism. Soc. Am.* **73**, 1527–1551.
- Gao, L. S., L. C. Lee, N. N. Biswas, and K. Aki (1983). Comparison of the effects between single and multiple scattering on coda waves for local earthquakes, *Bull. Seism. Soc. Am.* **73**, 377–390.
- Hanks, T. C. (1982). f_{max} , *Bull. Seism. Soc. Am.* **72**, 1867–1880.
- Haskell, N. (1960). Crustal reflection of plane *SH* waves, *J. Geophys. Res.* **65**, 4147–4150.
- Hudson, J. and J. R. Heritage (1981). The use of the Born approximation in seismic scattering problems, *Geophys. J. R. Astr. Soc.* **66**, 221–240.
- Kelly, K. R., R. W. Ward, S. Treitel, and R. M. Alford (1976). Synthetic seismograms: a finite difference approach, *Geophysics* **41**, 2–27.
- Malin, P. E. and R. A. Phinney (1984). On the relative scattering of *P* and *S* waves, preprint.
- Menke, W. (1983). A formula for the apparent attenuation of acoustic waves in randomly layered media, *Geophys. J. R. Astr. Soc.* **75**, 541–544.
- O'Doherty, R. F. and N. A. Anstey (1971). Reflections on amplitudes, *Geophys. Prospecting* **19**, 430–458.
- Papageorgiou, A. S. and K. Aki (1983). A specific barrier model for the quantitative description of inhomogeneous faulting and the prediction of strong ground motion. I. Description of the model, *Bull. Seism. Soc. Am.* **73**, 693–722.
- Richards, P. G. and W. Menke (1983). The apparent attenuation of a scattering medium, *Bull. Seism. Soc. Am.* **73**, 1005–1022.
- Sato, H. (1977). Energy propagation including scattering effects single isotropic scattering approximation, *J. Phys. Earth* **25**, 27–41.
- Simpson, D. W., M. W. Hamburger, V. C. Pavlov, and I. L. Nersesov (1981). Tectonics and seismicity of the Toktogul region, Kirgizia, USSR, *J. Geophys. Res.* **86**, 345–358.
- Waller, J. A. and P. E. Malin (1983). Shallow vertical seismic profile observations of earthquake wave attenuation (abstract), *EOS* **64**, 751.
- Wu, R.-S. (1982). Attenuation of short period seismic waves due to scattering, *Geophys. Res. Letters* **9**, 9–12.

SEISMOLOGICAL LABORATORY
 CALIFORNIA INSTITUTE OF TECHNOLOGY
 PASADENA, CALIFORNIA 91125
 CONTRIBUTION NO. 4079

Manuscript received 17 May 1984